

# 3D Radiative MHD Modeling of Particle Beam Heating of the Solar Atmosphere



Samuel Granovsky<sup>1</sup>, Alexander G. Kosovichev<sup>1</sup>  
<sup>1</sup>Department of Physics, New Jersey Institute of Technology



## 1 Background and Motivations

Solar flares release vast energy across the EM spectrum; However white-light flares (WLFs) are not entirely understood.

### Standard Model (Thick-Target Framework)

- Accelerated electrons travel from the corona to chromosphere.
- Energy deposited via collisions results in heating + hydrodynamic response.

### Problem

- Models predict heating mainly in upper chromosphere and weak photospheric response.
- Photospheric observations of WLFs (SDO HMI) reveal strong continuum brightening, Fe I 6173 Å line-core emission, and Helioseismic signals (sunquakes).

**Key Question: Can electron beams modeled in realistic 3D atmospheres produce the deep heating required to explain observed white-light emission and other photospheric effects?**

September 6, 2017 X9.3 White-Light Flare

### HMI Continuum: AR 12673

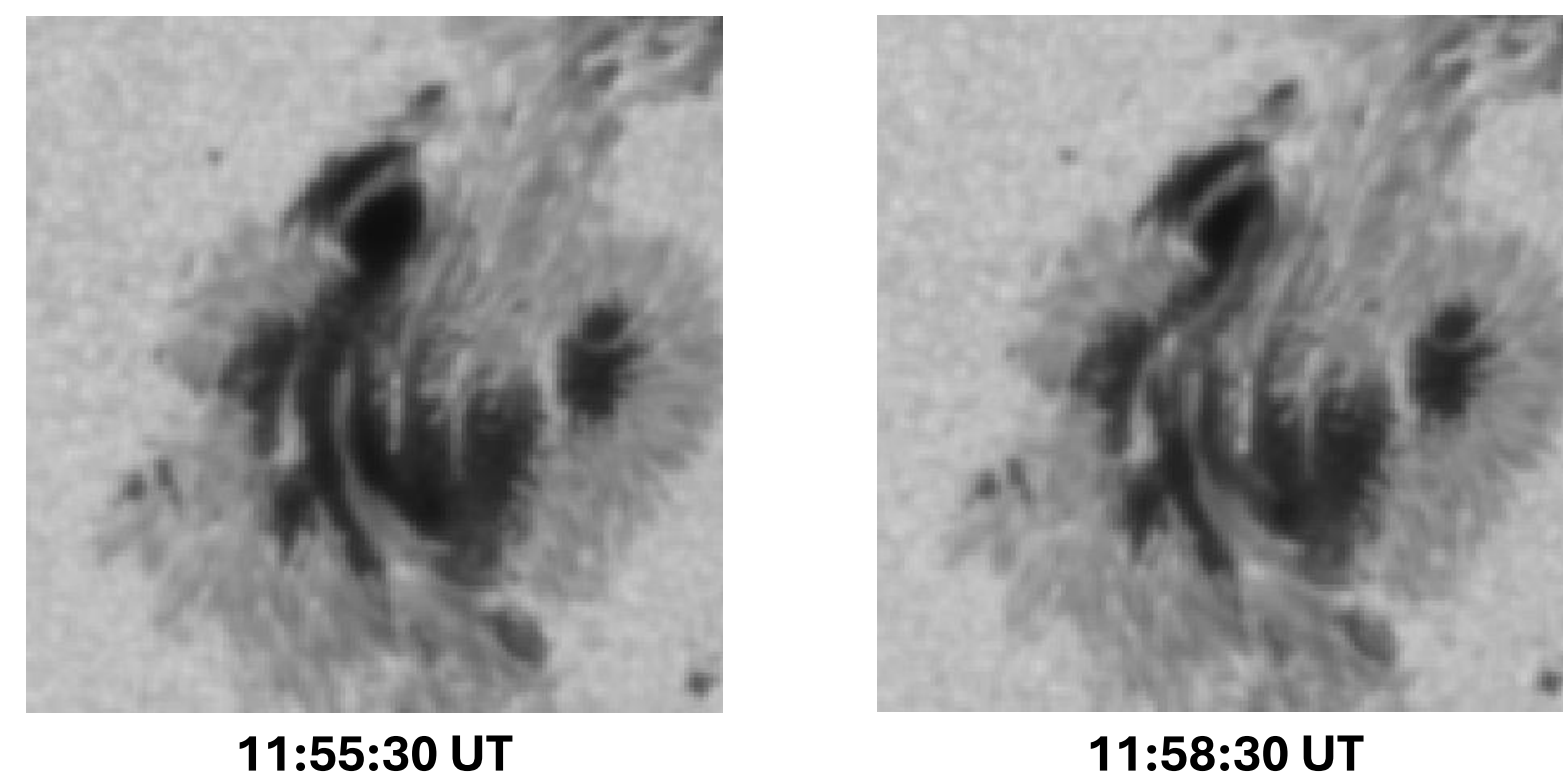


Figure 1a: HMI Continuum images of AR 12673 just before (left) and during (right) the 2017-09-06 flare

### HMI Stokes I vs Time (3 Locations)

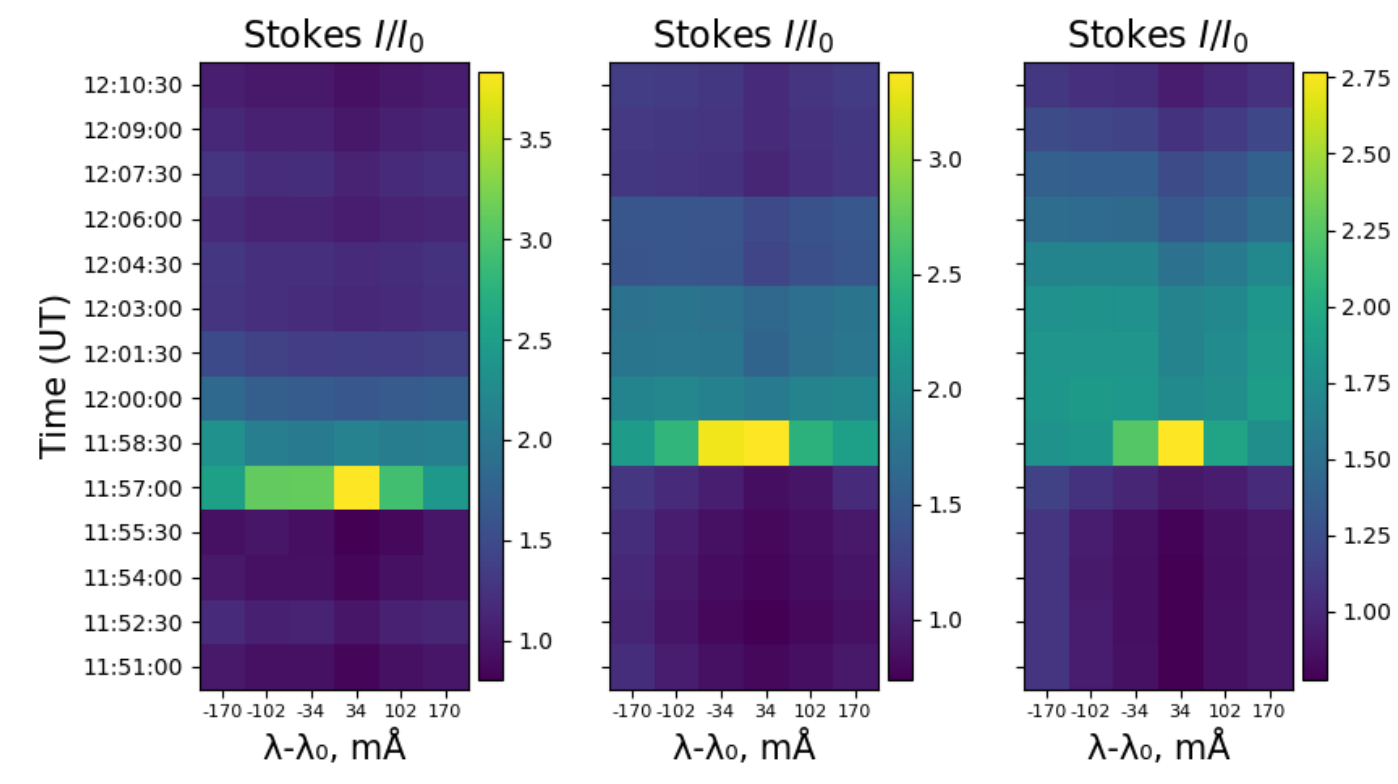


Figure 1b: HMI 6173 Å (Stokes I) intensity vs wavelength vs time during the 2017-09-06 Solar Flare at 3 locations in the active region.

## 2 Methods

### 3D Radiative MHD Simulations

- StellarBox code: 3D radiative magnetohydrodynamics (MHD) code that self-consistently models solar convection, magnetic fields, and radiative transfer, producing realistic, self-consistently evolving solar atmospheres from the subsurface to the corona.
- Domain:
  - Subsurface to corona ( $z = -10$  to  $+15$  Mm)
- Beam parameters:
  - Energy flux  $E_f = 10^{12} \text{ erg s}^{-1} \text{ cm}^{-2}$
  - Spectral index  $\delta = 3$
  - Low-energy cutoff  $E_c = 10\text{--}25 \text{ keV}$

### Beam Implementation

- Prescribed thick-target heating
- Vertical injection from top of domain
- Time-dependent, spatially localized beam

### Spectral Diagnostics

- Code: RH 1.5D
- Synthetic observational data:
  - Fe I 6173 Å line (HMI observable)
  - Full Stokes profiles

### Comparison Baseline

- 1D models: RADYN (F-CHROMA grid)

## 3 StellarBox: Atmospheric Response

### What we see in 3D:

- Strong heating primarily in the lower corona and upper chromosphere
- Formation of multiple shock fronts, chromospheric condensations, and bubble-like structures.

### Dynamics:

- Fast coronal shocks up to  $\sim 800 \text{ km/s}$  and rapid lateral expansion.
- Limited energy deposition below  $z = 1.25 \text{ Mm}$

### Effect of low-energy cutoff $E_c$ for fixed energy flux $E_f$ :

- Lower  $E_c$ : A larger number of electrons results in stronger heating higher in the atmosphere and earlier, more intense coronal shocks.
- Higher  $E_c$ : Fewer, more energetic electrons result in deeper penetration, heating at slightly lower heights, slower onset, and more localized chromospheric structuring.

**Even with high  $E_c$  beams, energy deposition remains too shallow to directly heat the photosphere.**

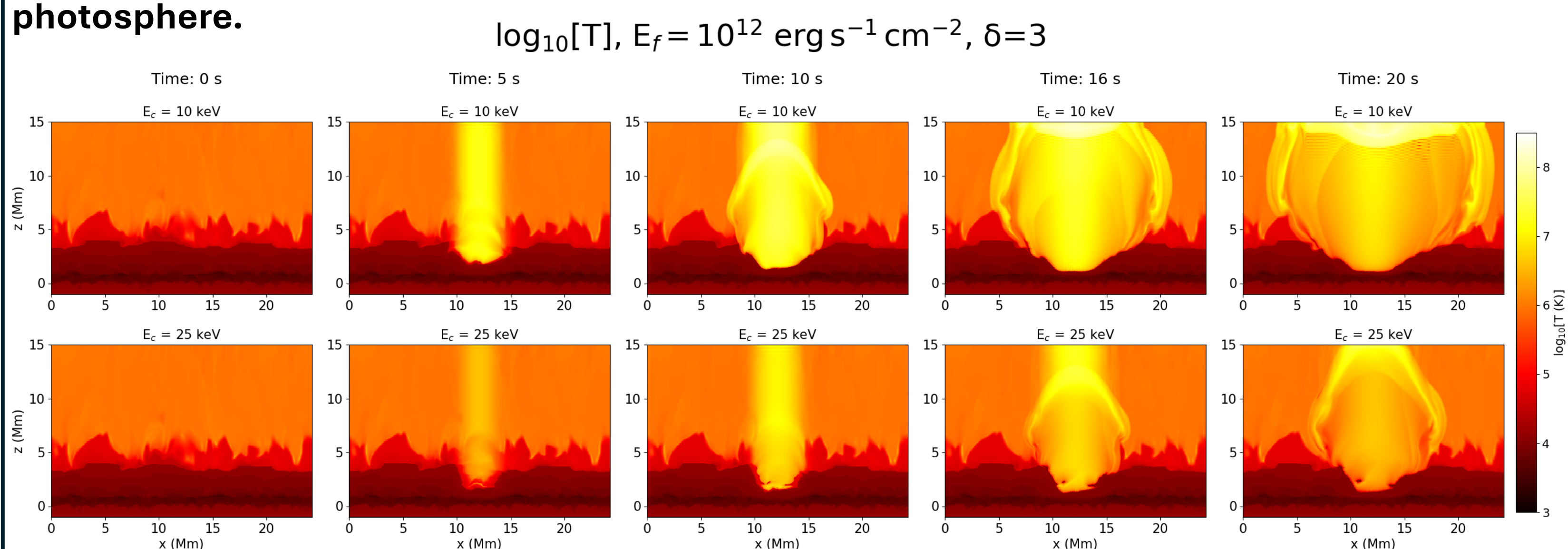


Figure 2: Vertical ( $xz$ ) slices of  $\log_{10}$  temperature ( $T$ ) vs time in 5 s intervals for the Stellarbox 10 keV beam case (top row) and the 25 keV case (bottom row). The slices are taken through the center of the beam.

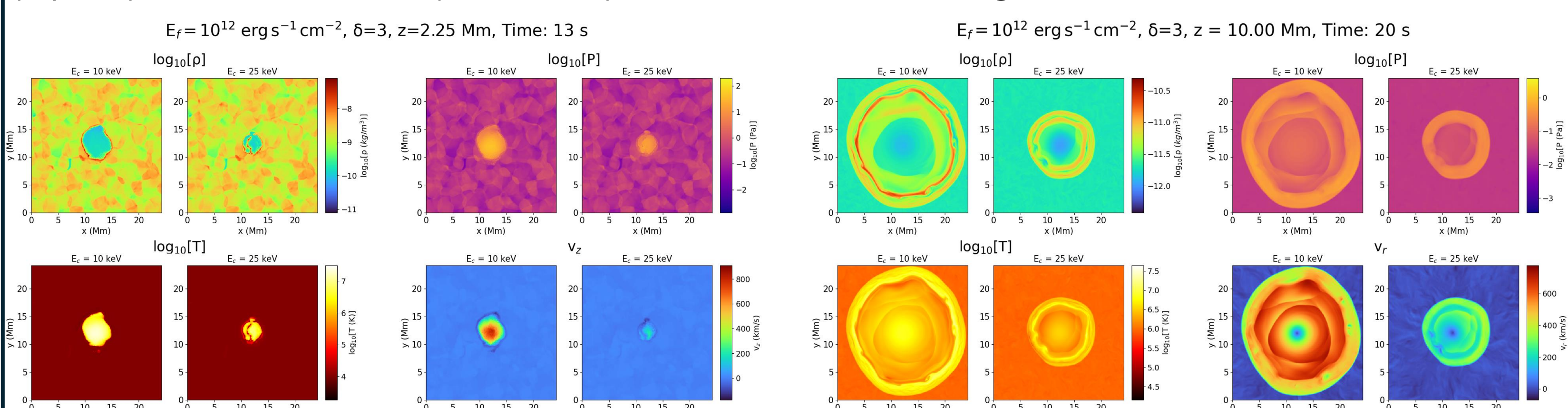


Figure 3a: Horizontal ( $xy$ ) slices of  $\log_{10}$  density  $\rho$  (top left),  $\log_{10}$  pressure  $P$  (top right),  $\log_{10}$  temperature  $T$  (bottom left), and vertical velocity  $v_z$  (bottom right) of the Stellarbox 10 keV beam case (left) and the 25 keV case (right) at  $z = 2.25 \text{ Mm}$ ,  $t = 13.0 \text{ s}$ .

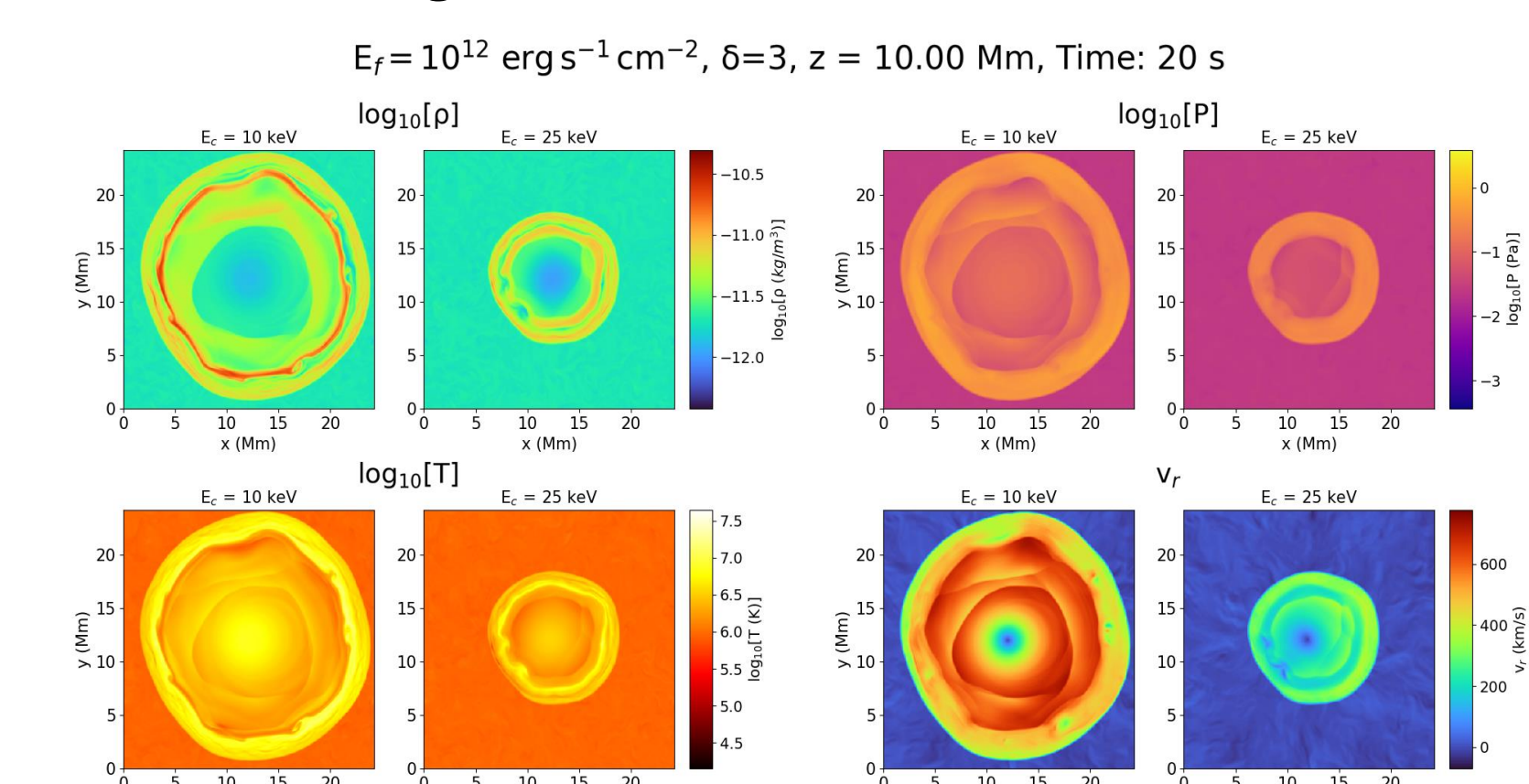


Figure 3b: Horizontal ( $xy$ ) slices of  $\log_{10}$  density  $\rho$  (top left),  $\log_{10}$  pressure  $P$  (top right),  $\log_{10}$  temperature  $T$  (bottom left), and horizontal / radial velocity  $v_r$  (bottom right) of the Stellarbox 10 keV beam case (left) and the 25 keV case (right) at  $z = 10.00 \text{ Mm}$ ,  $t = 20.0 \text{ s}$ .

## 4 Comparison: 3D StellarBox vs 1D RADYN Models

**Similarities:** Same dependence on beam energy cutoff, similar heating depths, and chromospheric heating + condensation reproduced.

**Differences:** 3D models show fine-scale structuring, faster heating, higher peak temperatures, and rapid cooling due to lateral expansion and multidimensional energy transport.

**Interpretation: Multidimensional transport significantly alters flare evolution, but not enough to deepen heating.**

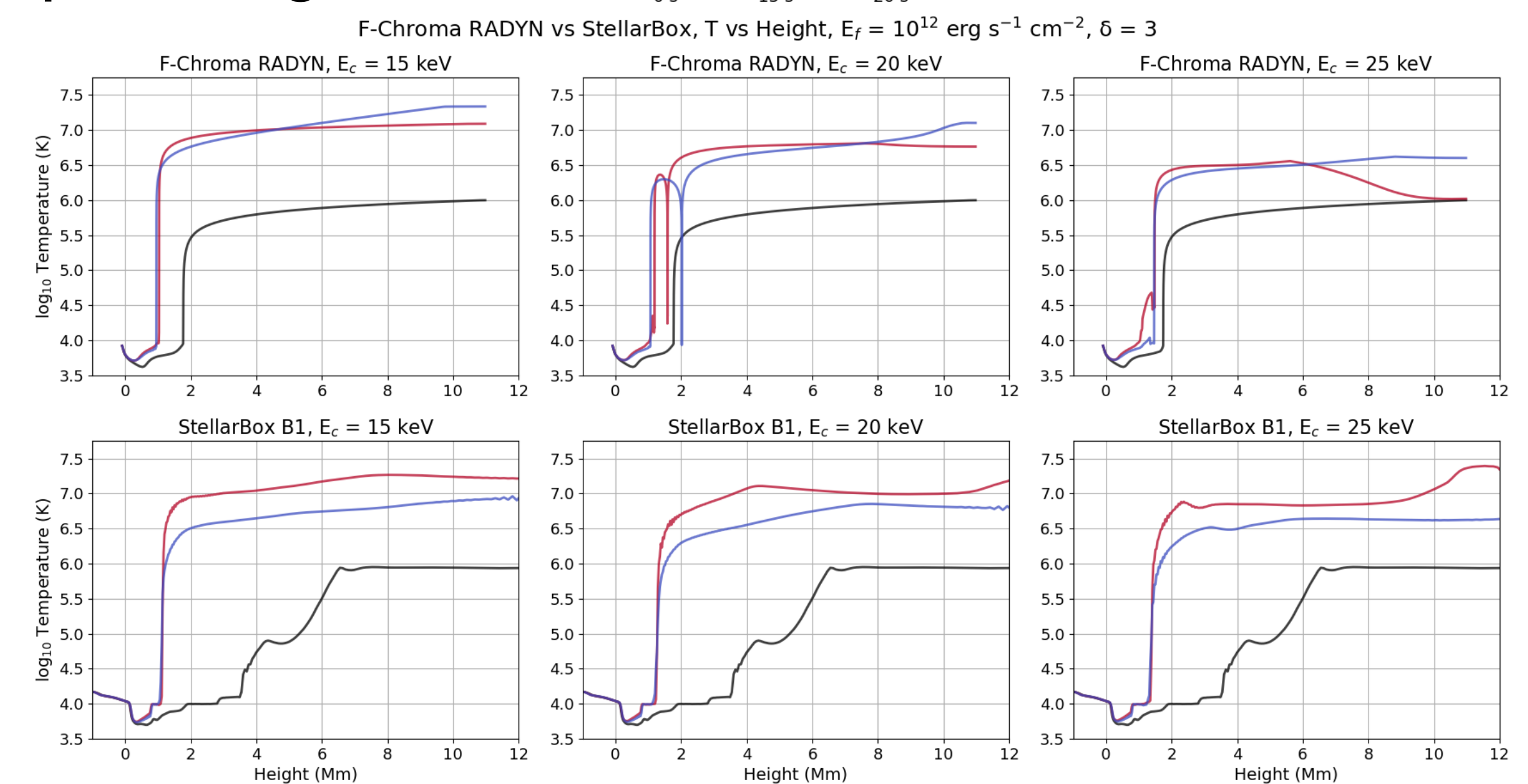


Figure 4:  $\log_{10} T$  vs height at  $t = 0 \text{ s}$  (black),  $15 \text{ s}$  (red), and  $20 \text{ s}$  (blue) for the 1D F-CHROMA RADYN 15, 20, and 25 keV models (top row) and the 3D Stellarbox 15, 20, and 25 keV models (bottom row). All beam parameters are identical.

## 5 RH 1.5D: Observable Signatures

### Continuum Emission:

- Enhancement up to **2.5x pre-flare levels**
- Comparable to observations of strong X-class WLFs
- Enhancement slightly stronger at higher  $E_c$

### Fe I 6173 Å Line Core:

- Line core reaches up to **97.8% of continuum intensity**
- Strong line-core brightening, however the line remains in absorption and does not reverse into emission as observed by HMI during some flares.
- Slightly stronger emission at higher  $E_c$

### Spatial Effects:

- Greatest continuum increase and line profiles closest to emission in / above **cooler regions** (intergranular lanes).

**Implication: Electron beams can explain continuum brightening, but not the full line-core emission seen in observations.**

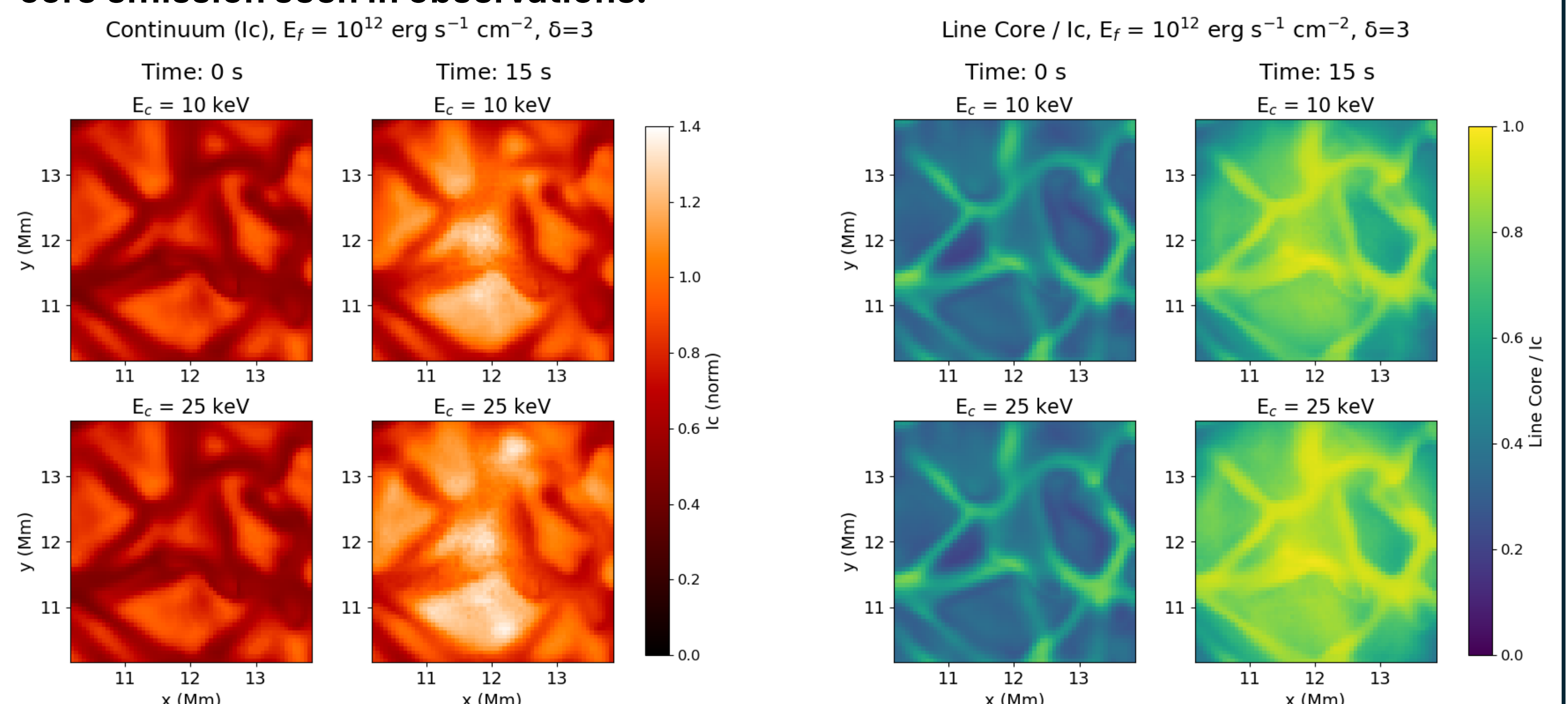


Figure 5a: Continuum intensity  $I_c$  at  $t = 0 \text{ s}$  (left) and  $t = 15 \text{ s}$  (right) for the Stellarbox 10 keV and 25 keV model (top) and 25 keV model (bottom).

Figure 5b: Line core /  $I_c$  at  $t = 0 \text{ s}$  (left) and  $t = 15 \text{ s}$  (right) for the Stellarbox 10 keV model (top) and 25 keV model (bottom). A value of 1 indicates the line core intensity is equal to  $I_c$ .

## 6 Interpretation and Implications

### Electron beams successfully reproduce:

- Strong continuum enhancements, dynamic chromospheric response

### Electron beams do not fully reproduce:

- Deep photospheric heating, full Fe I line emission, strong helioseismic impulses

### Likely missing physics:

- Deeper-penetrating particles (protons)
- Stronger magnetic fields (sunspot conditions)
- Field-aligned transport effects

## 7 Conclusions

### 3D radiative MHD models:

- Capture realistic structure and dynamics
- Improve over 1D models significantly

### Electron beams:

- Under realistic 3D conditions, electron beams fail to reproduce the depth of heating required for observed white-light flare kernels and fully account for previously observed photospheric flare signatures. This matches the thick target model and the results of previous work.

### White-light flare kernels likely require:

- Additional energy transport mechanisms
- Realistic active-region environments

## 8 Future Work

- Proton and mixed particle beams
- Strong-field (sunspot) atmospheres
- Field-aligned transport physics

**Goal: Fully explain white-light flare kernels and sunquake generation.**